Invited Paper

Holographic 3D fluorescence microscopy

David C. Clark[a], Changwon Jang[b], Jonghyun Kim[b], Byoungho Lee[b], and Myung K. Kim[a*]
[a]Dept. of Physics, University of South Florida, Tampa, Florida, USA
[b]School of Electrical Engineering, Seoul National University, Seoul, Korea
[*]Corresponding Author: mkkim@usf.edu

ABSTRACT

Fluorescence microscopy is an indispensable imaging tool in modern biomedical research. Holography is well-known to have many interesting and useful imaging capabilities. But the requirement of coherent illumination has all but precluded holography as a means for fluorescence imaging, which is inherently incoherent. Recent developments in digital holography, however, including self-interference incoherent digital holography (SIDH), provide highly effective and versatile capabilities for 3D holographic imaging with incoherent light, that can remove the barrier between fluorescence and holography. Recent progress in holographic fluorescence microscopy is presented.

Keywords: SIDH, differential imaging, fluorescence microscopy, incoherent holography, three-dimensional tracking, aberration, adaptive optics

1. INTRODUCTION

In conventional digital holography, interference pattern between object and reference beam is recorded as hologram. The information of object is carried in interference pattern. Propagation of generated hologram provides numerically reconstructed image of object based on diffraction theory [1]. The complex information of optical fields allows useful image processing techniques. However, need of coherence light limits the versatility of conventional digital holography. Therefore there have been efforts to alleviate the limitation by acquiring hologram with incoherent light [2,3]. Self-interference incoherent digital holography is one method of generating hologram from spatially incoherent light source such as LED light or even natural sun light [4]. Although conventional digital holography need reference beam in order to get interference pattern with object beam, in SIDH, the signal wavefront from object is duplicated with different curvature and then united again to generate interference pattern. Since the light source is spatially incoherent, interference pattern of each point source acts as point spread function and is superposed to generate hologram. Incoherent digital holography has remarkable advantage of versatility compared to conventional holography since incoherent light can be utilized to acquire the hologram of object. Especially, in this paper, we focus on fluorescence microscopy as application of SIDH.

2. EXPERIMENTS

A basic SIDH apparatus is represented in Fig. 1 [5]. It consists of the input lens, the relay lens, the interferometer, and a CCD array. The input lens produces an intermediate image as the input for the SIDH module. The relay lens is selected and positioned to create an appropriate final image space relative to the CCD plane (focal planes of interest should not fall directly on the recording plane for proper self-interference). The interferometer consists of a beam-splitting cube and two mirrors. One is a plane mirror mounted on a piezo-actuator for phase-shifting. The other is a curved mirror to generate differential phase curvature.

2.1 Broadband differential incoherent holography

The process of a basic differential SIDH is demonstrated with the case of chess pieces on a chess board illuminated by sunlight through an office window. This experiment is summarized in Fig. 2. The knight is moved from its initial position in FIG. 2(a) to a final position shown in Fig. 2(b and c). The difference hologram is calculated from the un-propagated initial and final complex holograms,

$$\Delta H = H_i - H_f \,. \tag{1}$$

Fifth Asia-Pacific Optical Sensors Conference, edited by Byoungho Lee, Sang-Bae Lee, Yunjiang Rao, Proc. of SPIE Vol. 9655, 96551M · © 2015 SPIE
CCC code: 0277-786X/15/$18 · doi: 10.1117/12.2185087

The difference hologram is shown in Fig. 2 (d-f) and contains the 3D optical field information of the knight in both initial and final positions, while the unchanged information, including the stationary king, are absent. As is shown, we shift the focus of each hologram from back knight to king to forward knight positions (Fig. 2 (a-c), respectively) and this information is preserved in the difference hologram (Fig. 2(d-f), respectively). It can also be noticed that the information on the chess board, both overlap and specular reflection of the knight, is also preserved in a difference hologram, since this represents changed information as well.

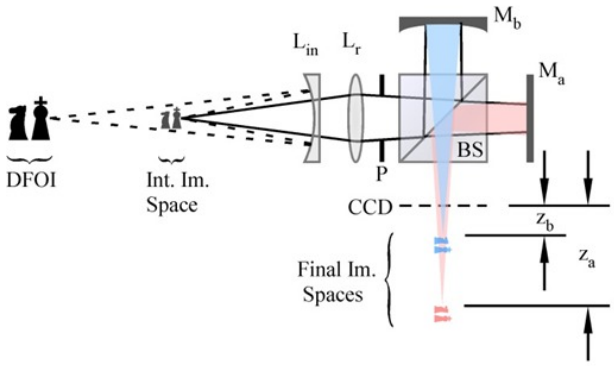

Figure 1. Experimental diagram for diff-SIDH. An input lens, L_{in}, projects objects in the depth field of view, DFOI, into the intermediate image space as input to the SIDH module. The SIDH module consists of a relay lens, L_r, an iris, P, a beam splitter, BS, a flat piezo-mounted mirror, M_a, a curved mirror, M_b, and a CCD camera.

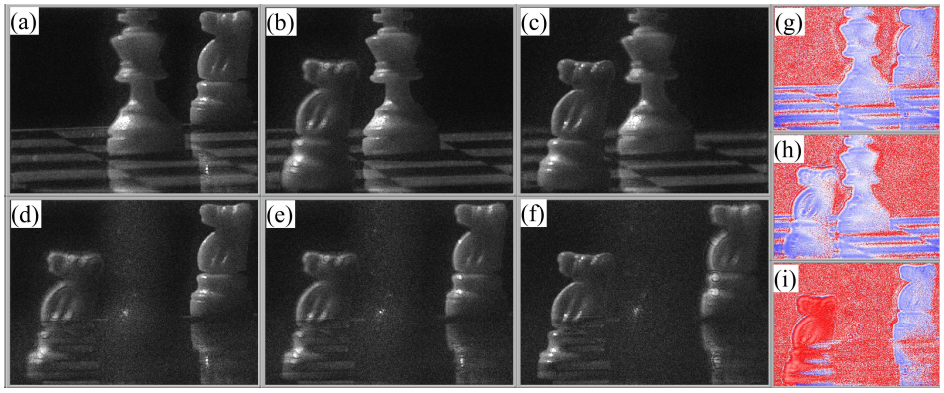

Figure 2. Summary of broadband differential incoherent holography experiment. Chess pieces, knight and king, were arranged as shown in the initial hologram, (a). The knight was then moved to a new position and a final hologram was recorded, (b) and (c). A difference hologram was computed from these and appears in (d), (e), and (f). Holograms (a) and (d) are propagated to the back knight plane, (b) and (e) are propagated to the king plane, and (c) and (f) are propagated to the front knight plane. (g), (h), and (i) are the phase images of the initial, final, and differential holograms showing a relative shift in the profile representing the final knight position.

2.2 Differential incoherent holographic microscopy

In preparation for working with fluorescence microscopy materials and instruments, we have fabricated a similar system to that above (Fig. 1) which we mount directly to the camera port of a standard commercial microscope. In essence, the input lens is replaced by the microscope as the input device to create the intermediate image space. In this way, the bright-field microscope images are successfully recorded here as complex holograms containing the 3D volumetric information of the object space extending above and below the microscope's normal input plane.

A slide containing a USAF1951 resolution target was placed on the microscope stage while a coverslip containing two particle-like structures was held approximately 8 mm above by a separate translation stage. The volume space was illuminated by a single color red LED (notably similar in incoherence and bandwidth to typical fluorescence emittance) and an initial hologram was recorded. The two-particle system was then translated laterally and a final hologram was

recorded. Just as above, a difference hologram was calculated resulting in a hologram containing only the two-particle system in its initial and final positions while all unchanged information from all planes is absent.

A summary of this experiment appears in Fig. 3. Figure 3(a-c) shows the amplitude representation of the initial, final, and difference holograms, respectively, all propagated to the resolution target plane. It is obvious in the difference hologram that this plane is now devoid of the resolution target information and that only the out-of-focus projections of the translated two-particle system are present. Meanwhile, Fig. 3(d-f) contain these same three amplitude holograms, but now propagated to the particle plane. At this plane, the two-particle system is clearly identified, in-focus, in the difference hologram at both its initial and final positions. As discussed in the previous experiment, a shift of complex information describes the initial and final positions of moved objects, although this is hidden in an amplitude representation. In this case, we display in Fig. 3(g-i) only the imaginary component of each of these same holograms and propagate them once again to the particle plane. In this representation, it is easy to detect the two particles, identified by circles for convenience, in their initial positions in Fig. 3(g), and their final positions in Fig. 3(h). More importantly, in Fig. 3(i), the final position of this two-particle system is shifted in this representation, clearly distinguishing it from the un-shifted initial position.

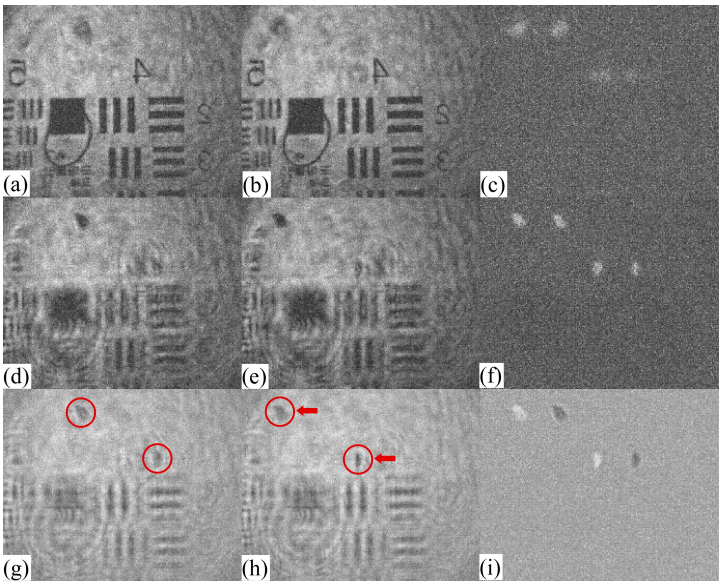

Figure 3. Summary of differential incoherent holographic microscopy experiment. (a), (b), and (c) are the initial, final, and differential holograms, respectively, all propagated to the resolution target plane. (d), (e), and (f) are the initial, final, and differential holograms propagated to the particle plane. (g), (h), and (i) are the imaginary component images of the initial, final, and differential holograms at the particle plane showing a relative shift (to white) in the profile representing the final particle positions.

2.3 Holographic fluorescence microscopy and aberration compensation

The imaging result of basic holographic fluorescence microscopy using SIDH technique without any aberration layer is presented in Fig. 4. Fig. 4 (a)-(b) shows amplitude and phase image of acquired complex hologram of the object. Fig. 4 (c) shows the numerically reconstructed image using angular spectrum method.

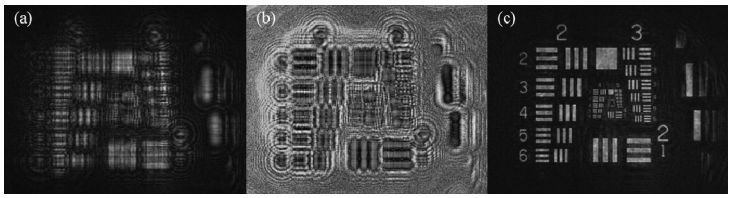

Figure 4. (a) Amplitude image and (b) phase image of the object hologram and (c) the reconstructed image from the hologram.

However, in presence of aberration layer, the wavefront is distorted and acquired hologram gives distorted image as well when reconstructed. Therefore guide star hologram is captured to measure and compensate the distortion caused by the aberration layer. Figure 5 shows amplitude and phase image of distorted holograms of the object and guide star. Without aberration layer, phase image of guide star hologram is expected to form a Fresnel zone plate pattern. However in Fig. 5 (d), distortion of hologram introduced by phase aberration can be observed. We performed image reconstruction by calculating the two dimensional correlation of object hologram and guide star hologram. The result is compared with the case of using conventional image reconstruction algorithm such as angular spectrum method as presented in Figure 6. Fig. 6 (a) is best focused image of hologram reconstructed by angular spectrum method varying the propagation distance. We can see that the image suffers from low contrast and severe distortion caused by aberration. On the other hand, Fig. 6 (b) is reconstructed result of proposed method, HFM with IDHAO, which shows remarkably enhanced image quality in contrast with the case of Fig. 6 (a). The complex point spread function which contains information of phase aberration is used to restore the original signal from distorted wavefront.

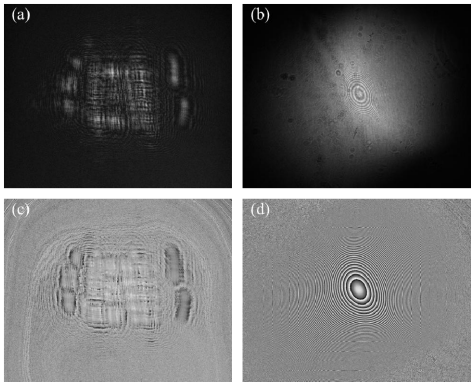

Figure 5. Amplitude images of (a) object hologram and (b) guide star hologram and phase images of (c) object hologram and (d) guide star hologram in presence of aberration layer.

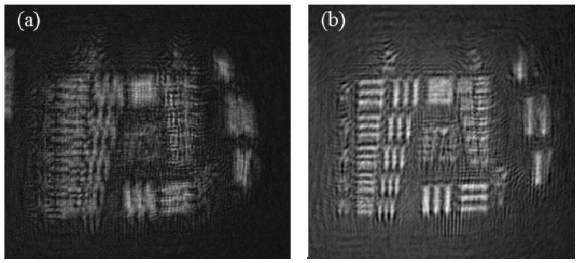

Figure 6. (a) Best focused image of reconstructed result using conventional method and (b) reconstructed result using IDHAO method.

3. CONCLUSION

We have described our development of a holographic fluorescence microscope that combines the three-dimensional imaging and tracking capabilities of differential SIDH with the versatile functional imaging by fluorescence microscopy. In addition, we are currently developing a single-shot, off-axis SIDH method which will eliminate the need for phase-shifting by incorporating a slight tilt between the self-interfering copies. We have also presented aberration compensation in HFM using SIDH. The adaptive optics by SIDH provides new tools for improved cellular fluorescence microscopy through intact tissue layers or other types of aberrant media.

REFERENCES

[1] Kim, M. K., “Principles and techniques of digital holographic microscopy,” SPIE Reviews 1(1), 018005 (2010).
[2] Lohmann, A. W.,“Wavefront reconstruction for incoherent objects,” J. Opt. Soc. Am. 55, 1555–1556 (1965).
[3] Dubois, F., Callens, N., Yourassowsky, C., Hoyos, M., Kurowski, P., and Monnom, O., “Digital holographic microscopy with reduced spatial coherence for three-dimensional particle flow analysis,” Appl. Opt. 45, 864–871 (2006).
[4] Kim, M. K., “Full color natural light holographic camera,” Optics Express 21 (8), 9636-9642 (2013).
[5] Kim, M. K., “Incoherent digital holographic adaptive optics,” Appl. Opt. 52, A117–A130 (2013).